Preliminary Experiment on the Plasma Confinement in the Heliotron Field with Buried Ring Conductors

By

Akihiro Mohri, Shinzaburo Matsuda and Koji Uo

In order to restore the plasma stability in the Heliotron C magnetic field, the Heliotron-P field, which has buried ring conductors inside the vacuum vessel and thus avoids the cusp losses, has been proposed. As a preliminary experiment on the plasma confinement in this field, the plasma behaviour in a mirror field having a current carrying ring conductor, which corresponds to the one section of the Heliotron-P field, is investigated. The plasma injected from a gun into this field rapidly fills up the region near the separatrix showing the existence of the magnetic well. The plasma ($T_e \simeq 20$ eV, $T_i \simeq 11$ eV, $n \leq 10^{11}$) is stably confined in this field. The predominant loss is the mirror end loss, and the net radial loss time is inferred to be 1.4 msec. Drift instability is observed only in the region of the steep density gradient at the plasma periphery.

1. Introduction

The Heliotron-C field[1],[2],[3] shown in Fig. 1.b provides the equilibrium of the plasma inside the separatrix, and the plasma with an appropriate density profile is stable for the flute instability. However, the experimental result on the Heliotron-C shows that the plasma produced by the ohmic heating does not have the above stable profile because of the rapid loss through the cusps.[4] In order to avoid the cusp loss and to restore the plasma stability, the Heliotron-P field (Fig. 1.a) which has the current carrying poloidal conductors inside the toroidal vacuum vessel, and the Helical Heliotron field which has the current carrying helical conductors inside the vessel were proposed.[4],[5],[6] The Heliotron-P field has also been called the Poloidal Heliotron field. Though the Heloitron-P field is the same as already proposed by Kadomtsev,[7] no one has yet performed the experiment on the plasma confinement in such a field.

These fields form the magnetic wells of the potential $U = -\int dl/B$, and the bottom of the well is on the separatrix.[7] As mentioned in the references (4) and (5), the plasma inside the separatrix does not contact with the supports of the buried
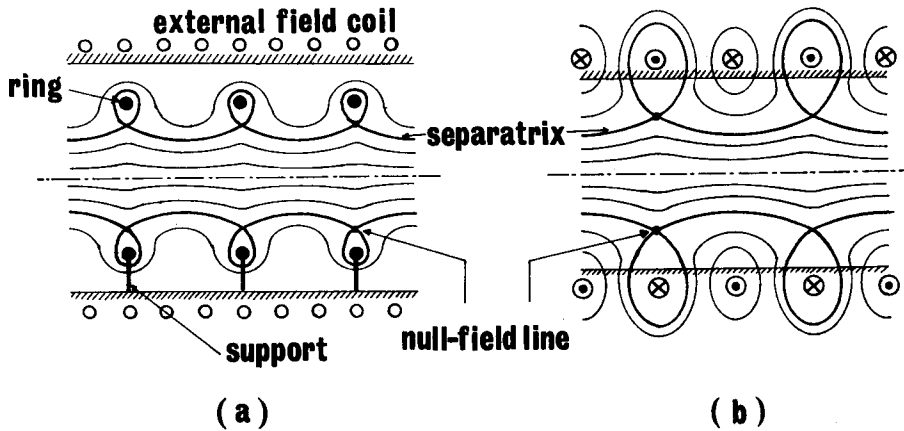
---

* Plasma Physics Laboratory

Fig. 1. Heliotron magnetic fields,
(a) Heliotron-*P* field.
(b) Heliotron-*C* field.

conductors and it is stable as far as the region just outside the separatrix is filled up by the plasma. When the plasma fills the region inside the maximum U surface, it is stable for flute instability. The plasma outside the separatrix will be lost gradually due to the support loss. Although the plasma inside the separatrix starts to leak out due to the flute instability when the plasma density just outside the separatrix becomes sufficiently low, we can decrease the effective loss rate by making the region inside the separatrix sufficiently wide compared with the size of the supports. Besides, if we compensate the plasma loss due to the supports by plasma injection or other means and keep the plasma density just outside the separatrix constant, the plasma inside the separatrix will be confined stably and the substitution of the old plasma by the newly injected plasma will take place only in the region outside the separatrix, but not inside it.

In this paper, a preliminary experiment on the plasma confinement in the magnetic field as shown in Fig. 2, which is the one section of the Heliotron-*P* field, is described. This is the combination of a usual mirror field and the magnetic field generated by an azimuthal ring current flowing on the midplane of the mirror field. The plasma is produced by gun injection in order to make the low-β plasma trapping and particles of sufficiently long mean free path. The existence of the minimum average B is verified by the observation of the injected plasma behaviour. In the previous report[4], detailed radial motions of the plasma in the stage of the plasma injection were not described. Besides, the reliable estimation of the radial loss of plasma was not made because of the lack of experimental data on the end loss of the plasma, and the fluctuation existing in the plasma was not identified.

The experiment described in this paper is carried out to elucidate the detailed loss mechanism of the plasma confined in the Heliotron-P field and also to identify its fluctuation observed at the plasma periphery.   The net radial loss of particles is estimated to be more than 45 times the Bohm confinement time by the direct measurement of the mirror end loss and the losses towards the ring and its supports. Density fluctuations and their identification are discussed.   It is also examined how the plasma behaves when the property of the minimum average B is removed.

2. Experimental Apparatus

A schematic diagram of the experimental setup is shown in Fig. 2.   The external mirror field is generated by six coils (31.6 cm diameter) and two auxiliary coils (24.4 cm diameter).   The axial length of the mirror field is 60 cm and its mirror ratio on the axis 1.74.   A vacuum vessel of the 15 cm diameter glass tube is placed under the mirror coils.   On the midplane of the mirror field, a copper ring is mounted whose major and minor diameters are 9 cm and 5 mm respectively. The current of the ring is externally supplied through a coaxial conductor, which forms a leg of two supporting rods of the ring.   The diameter of each support is 1 cm and they are fixed to the inner surface of the glass tube with rubber cushions. These coils and the ring are energized by the discharge of a capacitor bank of 63 kJ.   A current transformer is connected in series with the discharge circuit and
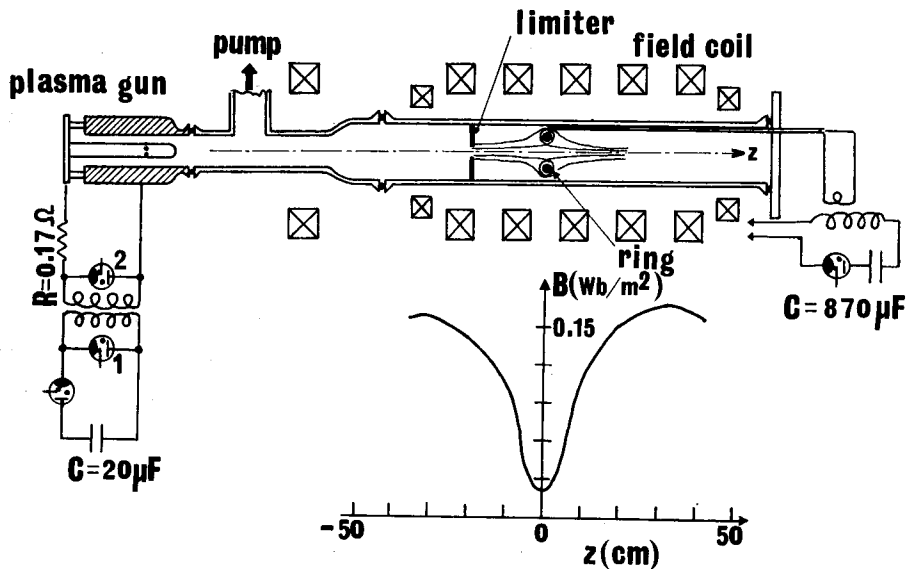

Fig. 2.   Schematic diagram of the experimental aparatus.   The magnetic field strength on
the axis is also shown as a function of the axial length z from the ring.

its secondary current is fed to the ring. The superposition of the external mirror field on the magnetic field produced by the azimuthal ring current forms a mirror field with a minimum average B configuration. The magnetic lines of force and the magnetic flux density on the axis are shown in Fig. 2. A quarter period of the field is 4.5 m sec and the null-field circle is located at 2.5 cm from the axis. The mirror ratio on the axis is 8.1. The magnetic flux density is normally 2.2×10^{-2} Wb·m^{-2} on the axis under the ring, and the maximum flux density on the axis is 0.18 Wb·m^{-2}.

A coaxial plasma gun consists of an aluminium outer electrode of 7.5 cm inner diameter and a copper inner electrode of 4 cm outer diameter. A fast acting valve for gas inlet is operated by electromagnetic repulsive force. The capacitor bank of the gun has 20 μF capacity and is normally charged to 15 kV. Its discharge circuit has double clamping ignitron switches as shown in Fig. 2. The switch 1 is used for usual clamping and the switch 2 controls the pulse duration of the gun current with the aid of a damping resistor of 0.17 $\varOmega$. The normal pulse duration is 40 μ sec. The helium plasma blob from the gun has the velocity of 5×10^{6} cm sec^{-1} corresponding to the ion energy of 52 eV. The plasma blob is guided by an axial magnetic field and injected into this magnetic trap through a glass aperture limiter placed at the mirror end. Three different limiters are used; limiter with aperture of 15 mm diameter, limiter having 3 mm wide circular slit of 5 cm diameter, and limiter with aperture of 3 cm diameter. These limiters have a function to reduce the influx of neutral gas from the gun. The base pressure is 6×10^{-6} Torr, and at 0.4 m sec after the injection, the neutral gas pressure rises to 7×10^{-5} Torr.

The density and the electron temperature are measured by using double probles and/or single probes. The flux of escaping particles out of the mirror ends is measured by a directional twin probe.[8] The ion temperature is inferred from the ion saturation current flowing into a single probe. A multichannel spectrometer and an image converter camera also help the observations.

3. Experiment

3.A *Experimental conditions*

In order to perform the experiment on the plasma confinement in the minimum average B Heliotron field, the following conditions of plasma parameters are required.

(i) $\beta = p/(B^{2}/2\mu_{0}) \ll 1$,

(ii) relative permittivity of the plasma: $\kappa_{\perp} = 1 + nM/(\varepsilon_{0}B^{2}) \gg 1$,

(iii) mean free path of particles: $\lambda \gg$ machine length: L,

(iv) $\dfrac{\text{connection length}}{\text{Alfvén velocity}} = \tau_A < \text{growth time of flute instability: } \tau_F \simeq \left(\dfrac{n}{\nabla n}\dfrac{R}{v^2}\right)^{1/2}$,

(v)   ion Larmor radius $\ll$ clearance between the ring and the tube wall.

Where β is the ratio of the plasma pressure to the magnetic pressure, M the ion mass, ε_0 the permittivity of vacuum, n the plasma density, R the average radius of curvature of the field line.   As mentioned in the following subsections, the plasma parameters after 250 μ sec from the injection are such that $n = 5 \times 10^{11}$, $T_i \simeq 50 \sim 10$ eV and $T_e \simeq 11$ eV.   Therefore, in this case, we obtain that $\beta \lesssim 10^{-3}$, $\kappa_\perp \simeq 2 \times 10^3$, λ_{i-i} (the ion-ion collision mean free path) $\approx 13 \sim 60$ m, λ_{e-e} (the electron-electron collision m.f.p.) 13 m, and $\tau_A \lesssim 9 \times 10^{-8}$ sec $< 2 \times 10^{-6}$ sec $\lesssim \tau_F$.   The conditions (i) to (iv) are all satisfied.   The clearance between the ring and the wall is 7 times the H_e^{++} Larmor radius at 20 eV.

3.B   Observations of the injection process

The plasma generated by the gun travels 55 cm and then spouts out through the aperture of the limiter into the trap field.   Some part of the plasma is impeded by the limiter, and it completely fades out during 150 μ sec after the gun firing. Then, the backward flow of plasma through the aperture is observed.   It is composed of the particles escaping from the trap region.   These phenomena are observed by using double probes put at several points near the aperture, and also by a movable directional twin probe.   This twin probe consists of two parallel molybdenum plates of 30 mm^2 area, and a glass insulator of 2 mm thickness is inserted between the plates.   The exposed surface of one plate faces to the upstream side and that of the other plate to downstream side.   Thus, the ion flow at the probe position can be estimated from the difference between the ion saturation currents into these plates, which are biased negatively against the plasma potential. The radial distributions of the axial plasma outflow at both the mirror ends are measured with the directional twin probe and their time variations are shown in Fig. 3.   On the limiter side, the plasma flow reverses its direction after 200 μ sec from the gun firing.

Since the bottom of the magnetic well is on the separatrix, the plasmas injected into the region apart from the separatrix will quickly fall towards the separatrix due to the flute instability.   To clarify this plasma motion, three different types of limiters shown in Fig. 4 are used.

The limiter of type A has a small aperture of 15 mm diameter, which does not enclose the separatrix.   The plasma injected through the aperture is initially localized inside the separatrix, and then it quickly spreads out towards the separatrix with
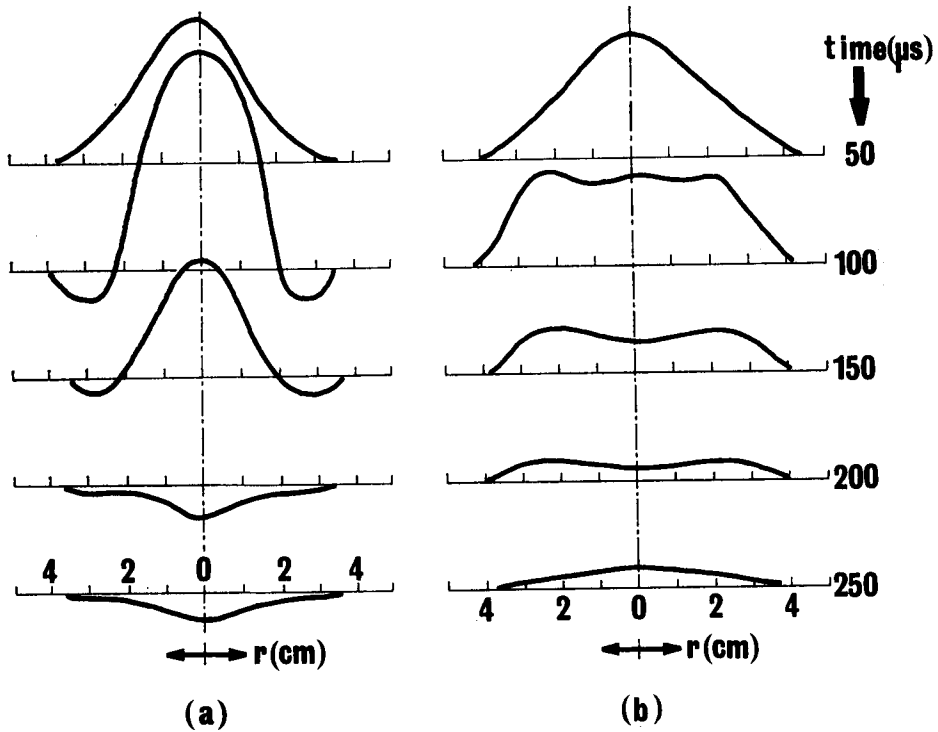
(a) **(b)**

Fig. 3.   Radial distribution of the axial particle flux.   The upper ordinate corresponds to
the flow in the positive z-direction of Fig. 2.
(a) At the mirror end of the limiter side.
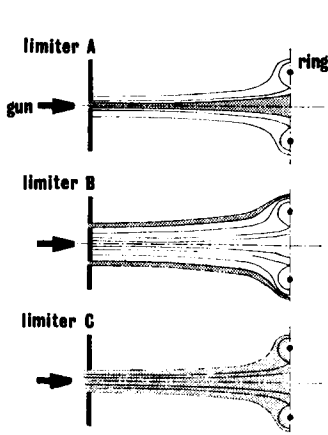(b) At the opposite mirror end.

Fig. 4.   Three types of limiters
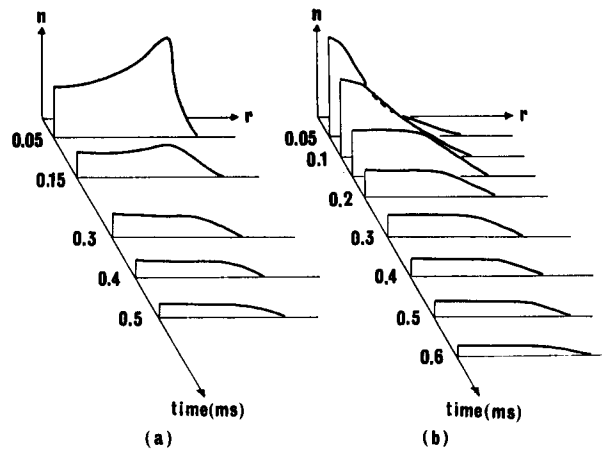used in the experiment.

Fig. 5.   Time variations of the radial density profile of the
plasma injected through the limiters.
(a) Through limiter B having a circular slit.
(b) Through the limiter C having an aperture of
3 cm diameter.

fluctuations of large amplitude. The velocity of the plasma spreading is in-sensitive to the magnetic flux density and about 2×10^5 cm/sec^{-1}. The growth rate of the flute instablility is given by

$$Im\omega = V_i\{(\nabla n/n)/R\}^{1/2} \tag{1}$$

where R is the average radius of curvature of the field line, which is given by $R = \oint \nabla B \, dl/|B|\oint dl$. In this case, $R = 7$ m, $(\nabla n/n)^{-1} = 1$ cm, and $v_i = 5 \times 10^6$ cm·sec^{-1}, whence $(\nabla n/n)^{-1}$ Im ω is estimated to be 2×10^5 cm·sec^{-1}, which agrees with the observed velocity.

On the other hand, the plasma injected through the limiter of type B, which has a circular narrow slit of 3 mm width at $r = 2.5$ cm outside the separatrix, falls towards the separatrix at the speed of 6×10^5 cm·sec^{-1}. Since $R = 37.5$ cm, we have the velocity of 1.1×10^6 cm·sec^{-1} for the flute instability, and the velocity is also of the same order as the observed velocity. If the particle injected through the limiter keeps its magnetic moment constant, it will easily escape through the other end of the mirror field. The occurrence of this instability may promote the trapping of plasma by breaking the adiabaticity of magnetic moment of particles. The radial density profiles after the gun firing are shown in Fig. 5(a). After 250 μ sec from the injection, the plasma is very quiescent and its radial density profile becomes flat across the plasma column. At the periphery, it has a steep gradient. The plasma decays with time reserving this density profile. From these experiments using the limiters of type A and B, it is clarified that the magnetic field has certainly its magnetic well on the separatrix. In the experiments described in the later section, the limiter of type C is always used so as to trap the plasma of larger number of particles. Time variations of the radial density profile are shown in Fig. 5(b). After the injection, the plasma fills up the trap region with the velocity of 7×10^5 cm·sec^{-1}. This is somewhat slower than the velocity of the plasma in case using the limiters of type A and B. This phenomenon is probably due to the gentle gradient of the density or smaller $\nabla n/n$. Although the plasma is very noisy before 250 μ sec after the injection, it becomes very quiescent and the density profile becomes the same one as shown in Fig. 5(a).

3.C *Confinement time*

The quiescent stage of the plasma follows the filling transition as mentioned in the preceding subsection. The plasma is confined in the region around the ring being kept away from the wall of the vacuum vessel. Figure 6 shows a time integrated photograph of the side view of the plasma.
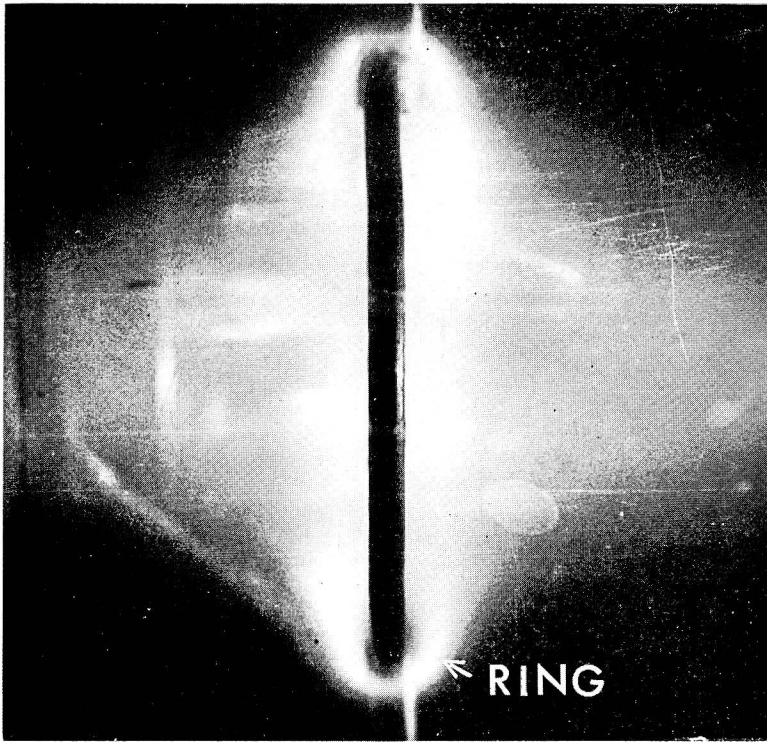
Fig. 6. A time-intergrated photograph of the side view of the trapped plasma.

A typical ion saturation current trace of the double probe is also shown in Fig. 7. The decaying plasma is very quiescent, though small density fluctuations are observed only in the region of the large density gradient. Time dependences of the density, the electron temperature and the ion temperature are plotted in Fig. 8.

The over-all decay time of the density is about 490 μ sec, and the ion temperature decreases with a time constant of about 200 μ sec, which well coincides with the decay time due to the charge transfer of ions with neutral gas at the pressure 7×10^{-5} Torr. The electron temperature remains almost constant.

The over-all decay time τ_n is expressed by

$$\frac{1}{\tau_n} = \frac{1}{\tau_{ns}} + \frac{1}{\tau_{nE}} + \frac{1}{\tau_{nr}}, \qquad (2)$$

where τ_{ns} is the supports loss time, τ_{nE} the mirror end loss time and τ_{nr} the net radial loss time.

The end loss time is obtained from the flux F of the escaping particles through the mirror ends; namely
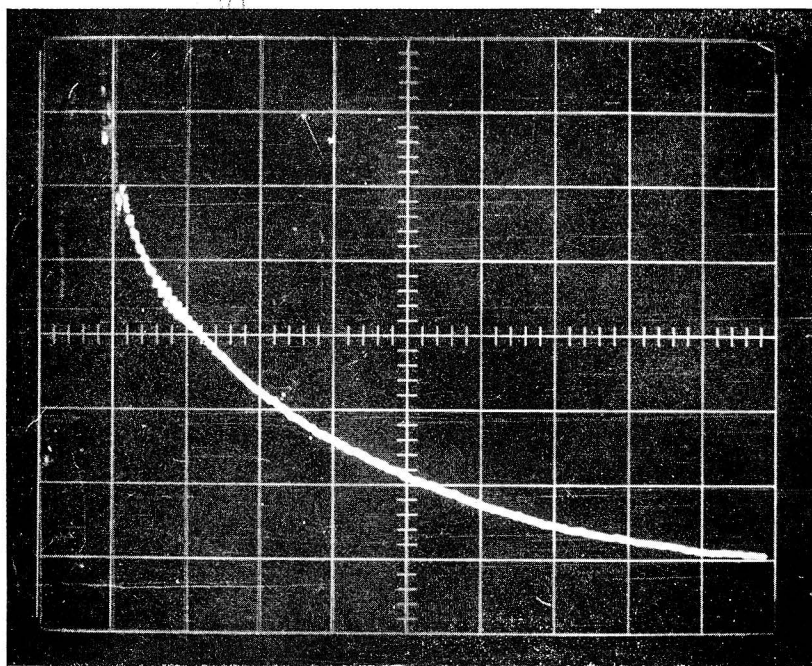
Fig. 7.   Ion saturation current trace cf the double probe put on the axis beneath the ring.
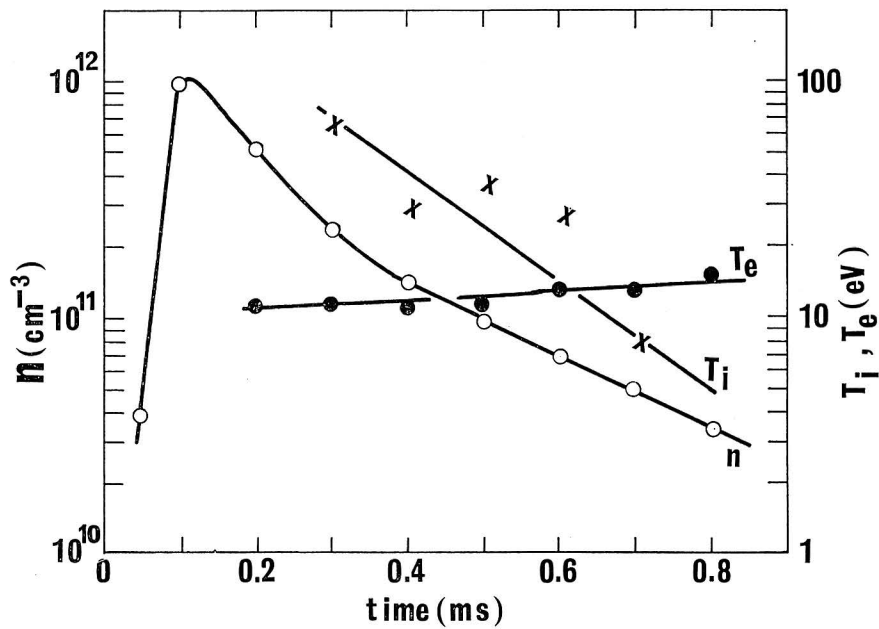Scanning speed： $100\,\mu\mathrm{sec/div}$.

Fig. 8.   Decay curves of density n, ion temperature T_i and electron temperature T_e of the helium plasma.

$$\tau_{nE} \simeq N/F \qquad (3)$$

where N is the total number of particles in the trap region at any given time. The flux F can be measured by using the directional twin probe, and also N is obtained from the density distribution over the trap region. At 400 μ sec after the gun firing, the measured τ_{nE} is about 910 μ sec (± 40 μ sec), which is comparable with the calculated mirror end loss time. It is likely that the null-field line acts as a scattering centre of particles in velocity space yieldidg the enhanced mirror end loss. However, it seems that this scattering effect is not dominant in this case.

The plasma loss time towards the ring and the supports, τ_{rs}, is measured by making them an ion collector. As a result, τ_{rs} is found to be 3.7~4.0 m sec.

Assuming the extreme condition that perfect recombinations between ions and electrons occur on the surface of the supports, we have the support loss time, τ_{ns}^{*}, as follows:

$$\tau_{ns}^{*} = \frac{V}{Sv_i}, \qquad (4)$$

where S is the effective cross section of the supports, v_i the thermal velocity of ions, and V the total volume of the trap region. Under the condition $T_i \simeq 20$ eV, we have τ_{ns}^{*} of 550 μ sec, which is shorter than experimentally obtained τ_{rs} by a factor 7.

The net radial loss time τ_{nr} is easily estimated from Eq. (3). Using the observed values of $\tau_{nE} \simeq 910$ μ sec and $\tau_{ns} \simeq 4$ m sec, finally we have $\tau_{nr} \simeq 1.4$ m sec. This time is about 45 times the Bohm time, $\tau_B = 2.8$ $r_p^2 B/T_e$ sec, which is given by assuming the radial density distribution of Bessel function $J_0(kr)$. Where r_p is the mean plasma radius in meter, B in Wb·m^{-2} and T_e in eV. The over-all decay time is 16 times τ_B.

3.D *Oscillations*

At the stage of the filling transition of the injected plasma, strong oscillations are observed, the frequency spectrum of which is like a white noise. After this stage, the plasma becomes very quiescent, although there exist density fluctuations of low frequencies around 20 kHz in the region of the large density gradient at the plasma periphery. Contrary, the fluctuations in the region of the flat density are of the magnitude less than 10^{-2}. Oscillations of high frequencies ranging from 160 kHz to 40 MHz are not observable all over the trap region.

Experimental results are summarized as follows. The measured values are taken on the plasma cross section apart from the ring by 13.5 cm.

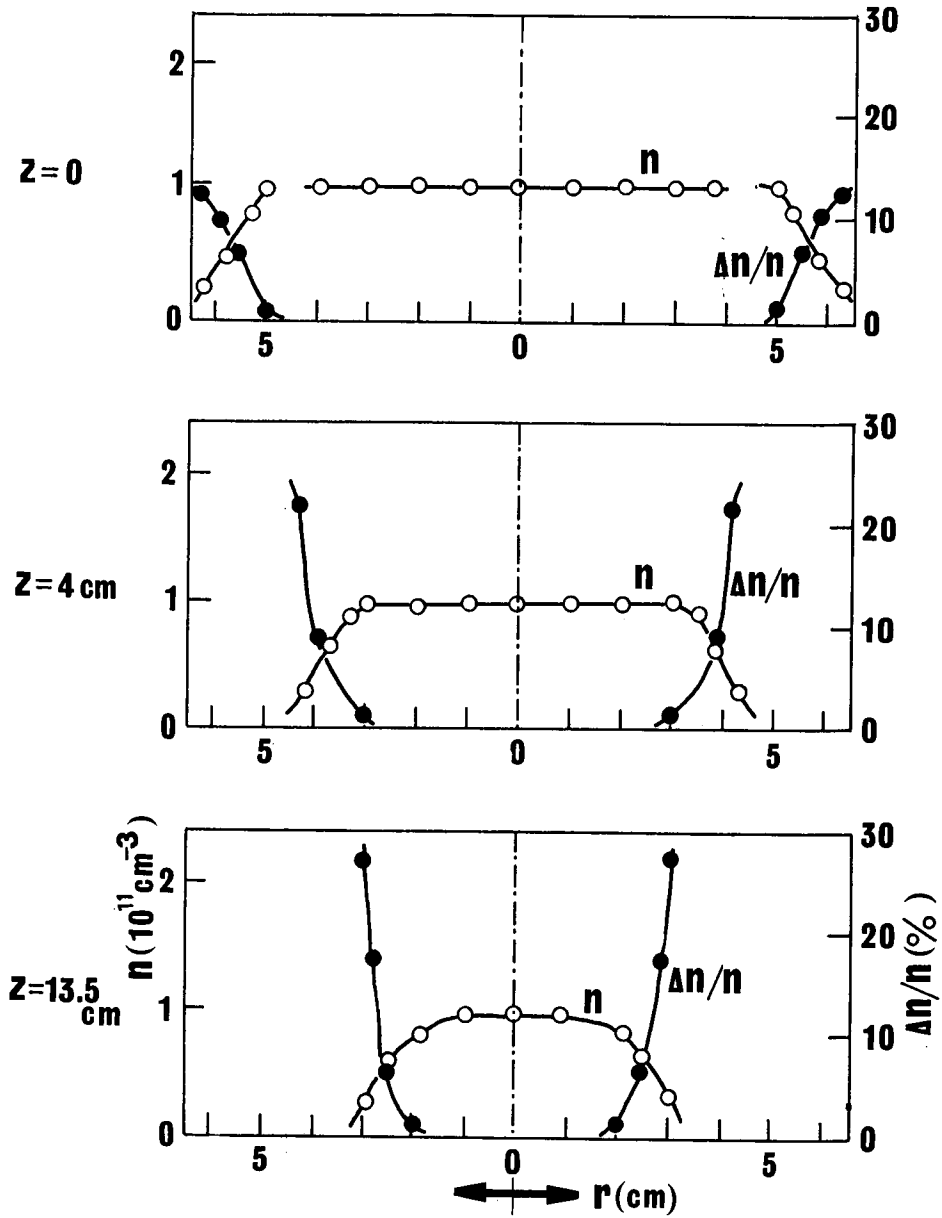(i) The oscillatory region is at the large density gradient as shown in Fig. 9.

Fig. 9. The region of the plasma fluctuation corresponding to the density profile. The probe
position from the ring is indicated by z.

(ii)   The frequency spectrum has a peak at 22 kHz.   Its secondary higher har-
monics of 45 kHz is also observable, but the reproducibility is not good.

(iii)   The wave number parallel to the field line, $k_{//}=2\pi/\lambda_{//}$, is nearly 10^{-1} cm^{-1},
since the parallel wave length $\lambda_{//}$ is twice the mirror length of 60 cm.

(iv)   The wave number perpendicular to the field $k_\perp = 2\pi/\lambda_\perp$ is 3 cm^{-1} which corresponds to the perpendicular wave length $\lambda_\perp$ of 2 cm or to the azimuthal wave number of 12.

(v)   The perpendicular phase velocity, $\omega/k_\perp$, is in the opposite direction of the diamagnetic currents.

(vi)   The perpendicular wave number $k_\perp$ increases from 2.0 to 3.6 cm^{-1} as the magnetic field rises from 0.12 to 0.18 Wb·m^{-2}.   The frequency ω slowly increases as the field becomes stronger as shown in Fig. 11.

(vii)   When the two glass plates are put at the both sides of the ring, as shown in Fig. 10, the oscillations stop if the distance L between the plates is shorter than 25 cm. The frequency becomes higher as L decreases.
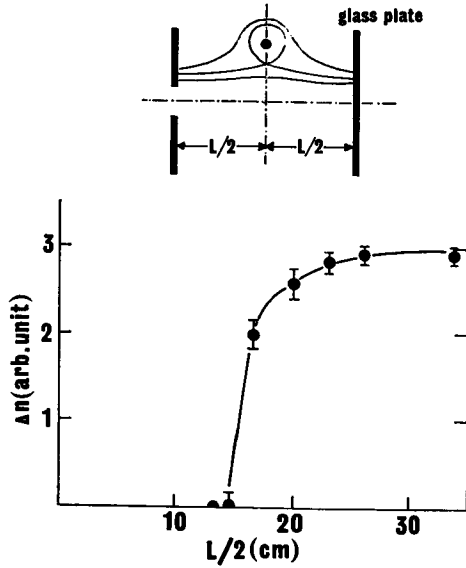

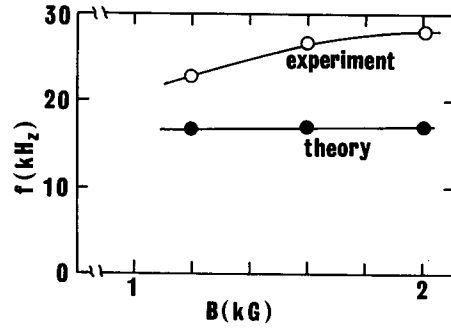Fig. 10.   Effect of the machine length on the fluctuations.

Fig. 11.   Frequency of the fluctuation with respect to the field strength.

(viii)   The radial density gradient at the plasma periphery becomes steeper as the magnetic flux density increases.

These measured properties of the fluctuation suggest that the oscillation is a drift wave instability, referring to the dispersion relations given by Krall and Rosenbluth[9].   Assuming that $T_{i\perp} \simeq T_{i\!/\!} \simeq T_i$ and $T_{e\perp} \simeq T_{e\!/\!} \simeq T_e$, and using the experimental data that $T_e \simeq 10$ eV, $T_i \simeq 20$ eV, $\nabla n/n = 2.6$ cm^{-1}, $k_\perp = 3$ cm^{-1}, $k_{\!/\!} \simeq 5 \times 10^{-3}$ cm^{-1} and the field curvature radius of -41 cm, we have $\omega \simeq 1.1 \times 10^5$ sec^{-1} or $f = 18$ kHz from the Eq (35) of Ref. (9).   The observed frequency is 22 kHz and it has a fairly good agreement with the theoretical value.   Similarly, the

observed dependence of ω on the magnetic flux density can be compared with the theoretical value as shown in Fig. 11.

The maximum length L_{max} for a device stable against drift instability was also found by Krall and Rosenbluth. In our case, $L_{max} = 12$ cm, which is about a half of the length obtained experimentally. (cf.(vii)). Since the probe used to detect the fluctuations has its tip length of 4 mm, the wave shorter than 4 mm could not be detected. Then, the length experimentally obtained may be longer than theoretical L_{max}. On the other hand, the marginal frequency at which $Im(\omega) = 0$ is also estimated to be 38 kHz, which is about twice the observed frequency 22 kHz. Thus, the observed fluctuations can be interpreted in terms of the drift instability, though there is a little discrepancy between the theory and the experimental results.
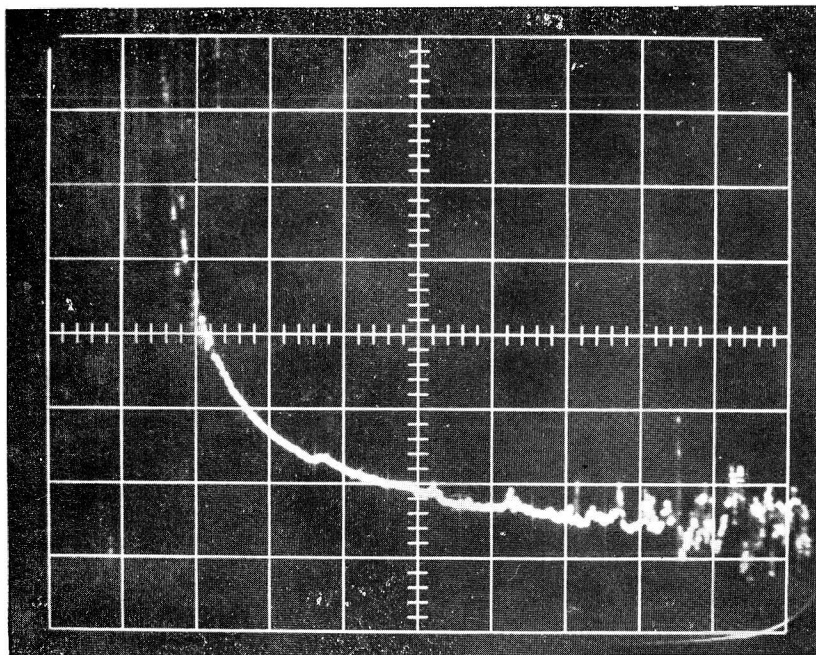

Fig. 12. Typical ion saturation current trace of the plasma in the Heliotron-C type field.
Scanning speed: $100\,\mu$ sec/div.

4. Distruction of Min B Property

A unit section of the Heliotron-C type field is produced by interposing a glass cylinder (25 cm long and 7 cm in diameter) inside the ring. All magnetic lines of force outside the separatrix cross the cylinder. Consequently, the property of minimum average B is destroyed. The conditions of the experiment are

kept unchanged.

Figure 12 presents a typical trace of the ion saturation current of the double probe, which is placed on the axis and 4 cm apart from the ring.   Strong density fluctuations last for a while, and then the relatively noisy decay follows.   The plasma density at the beginning of the latter stage is about one-tenth of that in case of the minimum average B.   Thus, it becomes evident that most of the injected plasma is lost at the early stage of the gun injection.   The successive density decay has a time constant of 300 μ sec, which is about two-thirds of the decay time in the minimum average B field.   At the latter stage of the decay, about 750 μ sec after the injection, a strong density fluctuation is always observed.   The mechanism of this instability is under investigation.

5. Summary and Conclusion

Preliminary experiment has been carried out on the plasma confinement in the one section of the Heliotron-P field, which is the magnetic mirror field having the property of minimum average B.   The field configuration is the combination of the mirror field and the magnetic field generated by the azimuthal ring current. The plasma parameters are selected so as to meet our experimental purpose, and the plasma is produced in the vacuum vessel by injection from the gun.   The radial motion of plasma injected from the gun shows that this magnetic field has certainly its magnetic well in the region about the separatrix.   The radial density profile at the quiescent stage of the plasma is flat in the most part of the plasma cross section except for the plasma periphery.   The over-all decay time is about 490 μ sec or 16 τ_B.   The net radial loss time of plasma, τ_{rr}, is inferred from the direct measurement of the end loss and the losses towards the ring and its supports. As a result, we have τ_{rr} of 45 τ_B or longer.   Since the end loss is predominant in this magnetic trap, detailed mechanisms of the net radial loss could not be discussed until an experiment on the toroidal machine with a train of this fundamental units is carried out.   The injected plasma after 250 μ sec from the gun firing is so quiescent as the density fluctuation is 10^{-2} or less in the region of the flat density profile, though the drift wave instability exists at the plasma periphery. Its perpendicular wave length is fairly short, so that it would not be fatal to the plasma containment.   The externally imposed helical field or the field generated by an axial current will be effective to suppress this instability by shear stabilization. Oscillations of higher frequency are not observable within the range of 160 kHz$\sim$ 40 MHz.

Acknowledgement

The authors would like to thank Prof. Y. Terashima and Prof. R. Itatani for the discussion concerning the identification of the instability. They are also indebted to Mr. M. Inoue for his assistance with the experiment.

References

1) K. Uo: Kakuyugo-Kenkyu, Circular in Japanese, **1** (1958) 1.
2) K. Uo: J. Phys. Soc. Japan, **16** (1961) 1380.
3) K. Uo, A. Mohri, H. Oshiyama, R. Kato and K. Ishii: Phys. of Fluids, **5** (1962) 1293.
4) K. Uo, R. Itatani, A. Mohri, H. Oshiyama, S. Ariga and T. Uede: Third Conference on Plasma Physics and Controlled Nuclear Fusion Research, CN–24/B–4 (1968).
5) K. Uo: Kakuyugo-Kenkyu, Circular in Japanese, **20** (1968) 193.
6) A. Mohri and S. Matsuda: Kakuyugo-Kenkyu, Circular in Japanese, **20** (1968) 165.
7) B.B. Kadomtsev: "Plasma Physics and the Problem of the Controlled Thermonuclear Reactions" (Pergamon Press, 1960), **4**, p. 417.
8) S. Ariga: Japan J. Appl. Phys., **7** 1968) 955.
9) N. Krall and M. Rosenbluth: Phys. of Fluids, **8** (1965) 1488.